Stiffness of serial and quasi-serial manipulators: comparison analysis

Alexandr Klimchik, Evgeni Magid, Stéphane Caro, Kriangkrai Waiyakan, Anatol Pashkevich

Stiffness of serial and quasi-serial manipulators: comparison analysis

Alexandr Klimchik[1], Evgeni Magid[1], Stephane Caro[2,3], Kriangkrai Waiyakan[4] and Anatol Pashkevich[2,5]

[1]*Innopolis University, Universitetskaya 1, 420500 Innopolis, The Republic of Tatarstan, Russia*
[2]*Institut de Recherches en Communications et en Cybernétique de Nantes, 1 rue de la Noe, 44321 Nantes, France*
[3]*Centre National de la Recherche Scientifique (CNRS), France*
[4]*Prince of Songkla University, 15 Karnjanavanich Rd., Hat Yai, Songkhla 90110, Thailand*
[5]*Ecole des Mines de Nantes, 4 rue Alfred-Kastler, Nantes 44307, France*

Abstract. The paper deals with comparison analysis of serial and quasi-serial manipulators. It shows a difference between stiffness behaviours of corresponding industrial robots under external loading, which is caused by machining process. The analysis is based on the estimation of compliance errors induced by cutting forces that are applied to the manipulator end-effector. We demonstrate that the quasi-seral manipulators are preferable for large-dimensional tasks while the quasi-serial ones better suit small size tasks.

1 Introduction

Enhancement of industrial robot performances extend their applications from traditional pic-and-place to operations where manipulator end-effector is subjected to essential external loadings [1]. They progressively take their niche in the drilling, milling, friction stir welding and other operations [2], [3], replacing more expensive CNC machines. Nevertheless, robot positioning accuracy under external loading is still an open high-demand research issue.

To improve robot accuracy under loading, there were developed different online and off-line error compensation methods [4]-[6], which allow reducing the impact of manipulator elasto-static deformations on the machining quality. The most efficient technique is based on the online tracking of robot position and compensation of related deflections. Another group of on-line methods is based on information from internal robot sensors; these methods could be implemented relatively easily and usually do not impose any restriction on the robot workspace. However, these methods require rather accurate geometric and stiffness models of the manipulator, which should be obtained case-by-case from the dedicated experimental study [7], [8]. The most essential limitation of the on-line approach is related to necessity of the manipulator model modification in robot controller software, which is usually not completely open for end-users. In contrast, the off-line error compensation technique does not require any intervention in the controller software, it is based on the modification of a target trajectory that is obtained using either a complete or a reduced manipulator model [9].

Another approach to improve manipulator accuracy under loading is based on mechanical methods, where the manipulator stiffness enhancement is achieved by means of closed loops, i.e. transforming conventional serial robots into quasi-serial ones. The most common way here is using gravity compensators, which in fact do not affect essentially manipulator stiffness. An alternative way is to use kinematic parallelograms [10], which potentially improve robot stiffness but require additional detailed investigations.

In classical robotics, robots are usually compared from their kinematic properties point of view. However, these performance measures do not suit well a manipulator under external loading since they are not able to take into account robot elasticity and influence of the external force which is applied to the manipulator end-effector. To overcome this difficulty, in robotics other performance measures were developed that are based on the norms of the stiffness matrix [11] or manipulator deflections at a specific "test pose" [12]-[14]. Nevertheless, they cannot be applied directly to the robot architecture comparison for machining application since they ignore some important technological issues. To overcome this difficulty, this paper proposes a new approach to comparison analysis of industrial robots, which is based on the compliance errors estimation for typical machining operations.

2 Problem of robot comparison

Typical *serial manipulators* contain robot base, robot arm and robot wrist (Fig. 1a). The robot base defines the arm orientation with respect to the robot world frame and

usually contains a single actuated joint providing rotation around z-axis. As shown in Fig. 1a, link #1 provides shifting of axis #2 with respect to axis #1. The robot arm is responsible for major movements of the robot end-effector. For 6-dof non-redundant robots, the translational movements are usually implemented using two actuated joints (joints #2 and #3). In anthropomorphic manipulators, these joints are also referred to as a robot shoulder and an elbow respectively. Corresponding links #2 and #3 define the manipulator workspace. The end effector orientation is achieved by the robot wrist. In the majority of manipulators, a robot wrist contains three revolute actuated joints (joints #4, #5 and #6) where joint axes intersect in a same point (a so-called *spherical wrist*). In a relevant geometric model, the wrist linear parameters may be omitted and included in the parameters which describe link #3 and the tool transformation. However, in practice, the robot can be equipped with a non-spherical wrist (e.g., an off-set wrist, a hollow wrist, etc.) whose geometrical model includes more parameters.

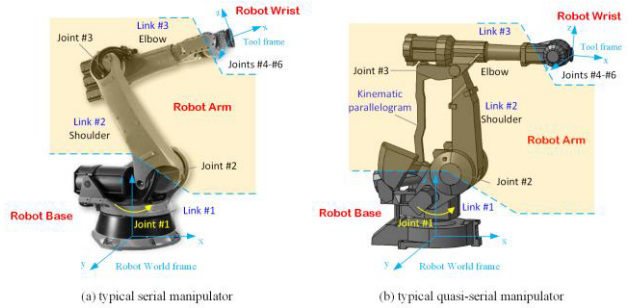

Figure 1. Architecture of typical industrial robots

Quasi-serial robots have roughly similar architecture (see Fig. 1b) but in contrast to their serial counterparts, a robot arm of a quasi-serial manipulator contains a kinematic parallelogram, which can be treated as an internal closed-loop. For this reason, such robots are often referred as quasi-serial ones. In practice, the kinematic parallelogram allows robot designers to increase robot dynamic properties by means of moving masses reduction (locating heavy actuating motor #3 on the robot base instead of a robot elbow). Usually, the parallelogram does not essentially affect manipulator control and does not change manipulator direct/inverse kinematic equations. On the other hand, the quasi-serial manipulator stiffness model essentially differs from its serial counterpart since re-location of the manipulator compliant element (actuator #3 transmission) essentially influences the stiffness behaviour [15]. For this reason, previous results, which are obtained for strictly serial manipulators cannot be directly applied in such case.

A stiffness model of a robotic manipulator (both serial and quasi-serial) describes the manipulator behavior under loading [16], [17]. In addition to the conventional robot parameters (i.e., geometric ones), it includes a number of elastic parameters which describe flexibility of the manipulator links and joints. In a number of industrial applications, the manipulator elasticity cannot be ignored since the high loading is applied to a robot, while the required positioning accuracy is rather high. For example, from our experience it is known that the end-effector deflection of heavy industrial robots under loading of 1kN may vary from 1 to 10 mm within the robot workspace, while demanded accuracy for the machining process is typically about 0.1 mm. These compliance errors can be reduced down to admissible level using both on-line and off-line error compensation techniques, which are based on the appropriate stiffness model [18], either “complete” or “reduced”. The complete stiffness model of an industrial robot is complicated and takes into account all manipulator links and actuators compliances [19] (Fig. 2a). In practice, a number of manipulator components may be treated as rigid ones (e.g., some links), while the main compliance is concentrated in the actuator transmissions. This allows us to apply so-called reduced models that take into account the joint elasticities only [20]. Such models are quite common for stiffness modeling of heavy industrial robots where the links are massive and their deflections under the force of 1kN are much lower than 0.1 mm. The reduced stiffness model is also quite useful at the design stage since it gives valuable approximation of the manipulator stiffness behavior, which is required for optimization. Moreover, in most cases these models could be used to compare stiffness properties of the manipulators of different architectures. For this reason, the presented in this paper comparison study is based on the reduced stiffness model.

To make the comparison comprehensible, let us perform further simplification of the considered models. At first, in the frame of the comparison study, it is possible to exclude the robot base from the stiffness analysis. It is obvious that this component influences the stiffness properties of both serial and quasi-serial manipulators in the same way. Further, since the wrist dimensions are essentially smaller than the lengths of the links #2 and #3, we simplify the model by excluding the robot wrist components.

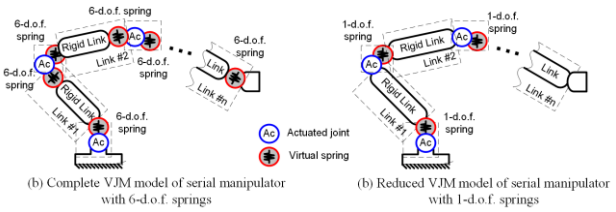

Figure 2. Complete and reduced stiffness models of an industrial robotic manipulator

3 Stiffness model of a serial manipulator

Let us obtain first the reduced stiffness model of a typical serial manipulator. The desired model takes into account the actuator compliances only, which usually are the most important elastic components of the entire manipulator. In the case of a serial manipulator, the robot arm contains two actuated revolute joints $q_2.q_3$ and two links of lengths l_2, l_3 (Fig. 3). It is worth mentioning that in some robots link #3 is described with two geometrical

parameters l_{3x}, l_{3y} (see Fig. 3). Nevertheless, these two parameters can be easily presented as a single link length $l_3 = \sqrt{l_{3x}^{\,2} + l_{3y}^{\,2}}$ and the joint offset $\Delta q_3 = atan2(l_{3y}, l_{3x})$.

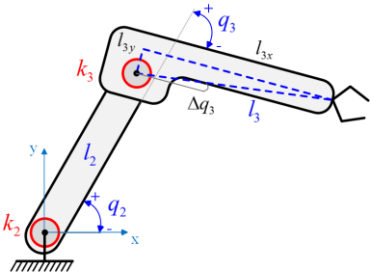

Figure 3. Kinematic structure and basic parameters of a serial robot arm

For the considered manipulator, the stiffness model contains two elastic parameters k_2 and k_3 describing compliances of corresponding joints. For this geometry, the Cartesian stiffness matrix $\mathbf{K}_C$ describes manipulator resistance to the external force $\mathbf{F}$, which is applied to the end-effector, and could be expressed as

$$\mathbf{K}_C = \left(\mathbf{J}_S \, \mathbf{k}_\theta \, \mathbf{J}_S^{\,T}\right)^{-1} \tag{1}$$

where the diagonal matrix $\mathbf{k}_S = diag(k_2, k_3)$ collects the joint compliances, and $\mathbf{J}_S$ is kinematic Jacobian. For the serial arm, the Jacobian matrix is presented as

$$\mathbf{J}_S = \begin{bmatrix} -l_2 \cos q_2 - l_3 \cos(q_2 + q_3) & -l_3 \cos(q_2 + q_3) \\ l_2 \sin q_2 + l_3 \sin(q_2 + q_3) & l_3 \sin(q_2 + q_3) \end{bmatrix} \tag{2}$$

where $l_2 . l_3$ are the link lengths, q_2, q_3 are the actuated joint coordinates. After relevant substitution and transformations, we obtain the following expression for the serial manipulator compliance $\mathbf{k}_C = \mathbf{K}_C^{-1}$

$$\begin{aligned} \mathbf{k}_{CS} &= \begin{bmatrix} k_{CS}^{(1,1)} & k_{CS}^{(1,2)} \\ k_{CS}^{(1,2)} & k_{CS}^{(2,2)} \end{bmatrix} \\ k_{CS}^{(1,1)} &= k_2 \left(l_2 \, c_2 + l_3 \, c_{23}\right)^2 + k_3 l_3^{\,2} \, c_{23}^2 \\ k_{CS}^{(1,2)} &= -k_2 (l_2^{\,2} \, c_2 \, s_2 + l_2 l_3 \, c_3 + l_3^{\,2} \, c_{23} \, s_{23}) - k_3 l_3^{\,2} \, c_{23} \, s_{23} \\ k_{CS}^{(2,2)} &= k_2 \left(l_2 \, s_2 + l_3 \, s_{23}\right)^2 + k_3 l_3^{\,2} \, s_{23}^2 \end{aligned} \tag{3}$$

where $c_2 = \cos q_2$, $s_2 = \sin q_2$, $c_3 = \cos q_3$, $s_3 = \sin q_3$, $c_{23} = \cos(q_2 + q_3)$, $s_{23} = \sin(q_2 + q_3)$. As follows from our experience, the joint compliances k_2, k_3 are quite close to each other and may be assumed to be equal, i.e. $k_2 = k_3 = k$. Besides, it is reasonable to introduce a ratio coefficient $\mu = l_3 / l_2$ which defines the ratio between the link lengths. This allows re-writing the compliance matrix in a more compact form

$$\mathbf{k}_{CS} = k l_2^{\,2} \begin{bmatrix} (c_2 + \mu c_{23})^2 + \mu^2 c_{23}^2 & -c_2 s_2 - \mu c_3 - 2\mu^2 c_{23} s_{23} \\ -c_2 s_2 - \mu c_3 - 2\mu^2 c_{23} s_{23} & (s_2 + \mu s_{23})^2 + \mu^2 s_{23}^2 \end{bmatrix} \tag{4}$$

which is convenient for the further comparison analysis.

4 Stiffness model of a quasi-serial manipulator

Applying a similar technique, let us obtain the reduced stiffness model of a quasi-serial manipulator. In contrast to its serial counterpart, the robot arm of the quasi-serial manipulator contains a kinematic parallelogram whose adjacent sides could be treated as the links #2 and #3 (Fig. 4). Besides, here the actuators are usually located at the same axis (corresponding to the joint #2 of the serial manipulator). Such kinematics is quite common in heavy industrial robots since it allows reducing the robot arm inertia and improving its dynamic properties. For comparison purposes, the geometric and elastic parameters of the quasi-serial arm are assumed to be the same as for the corresponding serial case.

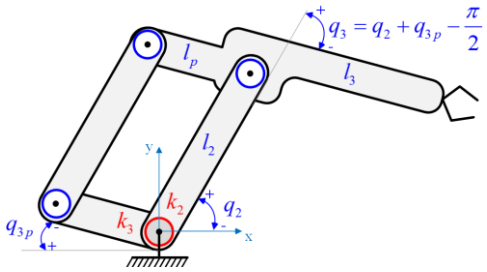

Figure 4. Kinematic structure and basic parameters of a quasi-serial robot arm

For the quasi-serial geometry, the desired stiffness matrix can be computed using expression (1), where the Jacobian should be replaced by

$$\mathbf{J}_P = \begin{bmatrix} -l_2 \cos q_2 & -l_3 \cos q_{3p} \\ l_2 \sin q_2 & l_3 \sin q_{3p} \end{bmatrix} \tag{5}$$

Here q_{3p} is the coordinate of the actuated joint #3, which differs from q_3 in the serial manipulator. Using this notations, the compliance matrix of the quasi-serial robot can be expressed as

$$\mathbf{k}_{CP} = \begin{bmatrix} k_2 l_2^{\,2} \, c_2^2 + k_3 l_3^{\,2} \, c_{3p}^2 & -k_2 l_2^{\,2} \, c_2 \, s_2 - k_3 l_3^{\,2} \, c_{3p} \, s_{3p} \\ -k_2 l_2^{\,2} \, c_2 \, s_2 - k_3 l_3^{\,2} \, c_{3p} \, s_{3p} & k_2 l_2^{\,2} s_2^2 + k_3 l_3^{\,2} s_{3p}^2 \end{bmatrix} \tag{6}$$

where $c_{3p} = \cos q_{3p}$, $s_{3p} = \sin q_{3p}$. Following the assumptions on the stiffness coefficients (i.e., $k_2 = k_3 = k$) and introducing the link lengths ratio $\mu = l_3 / l_2$, the above matrix can be presented in the compact form as

$$\mathbf{k}_{CP} = k l_2^{\,2} \begin{bmatrix} c_2^2 + \mu^2 c_3^2 & -c_2 s_2 - \mu^2 c_3 s_3 \\ -c_2 s_2 - \mu^2 c_3 s_3 & s_2^2 + \mu^2 s_3^2 \end{bmatrix} \tag{7}$$

Using the compliance matrices (4) and (7), it is possible to estimate the manipulator end-effector deflections under the given external loading (for a given robot configuration) and also to compare the manipulator stiffness behaviour and influence the link-length ratio on the force-deflection relation.

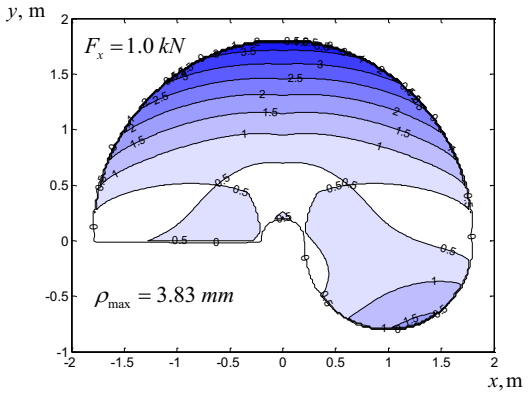

(a) Compliance map for *serial manipulator* under the external loading in x-direction

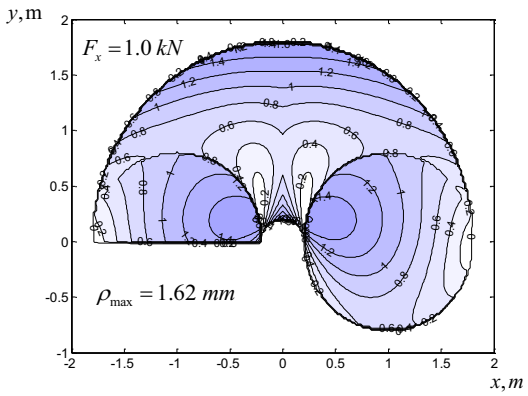

(b) Compliance map for *quasi-serial manipulator* under the external loading in x-direction

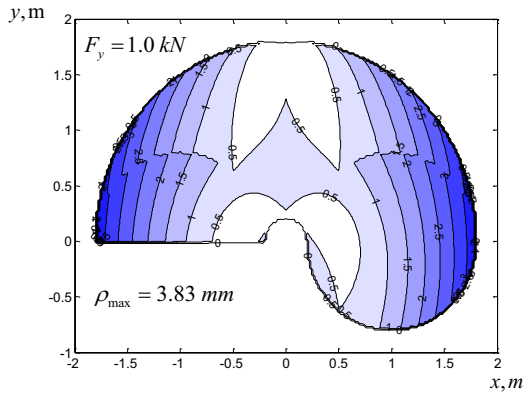

(c) Compliance map for *serial manipulator* under the external loading in y-direction

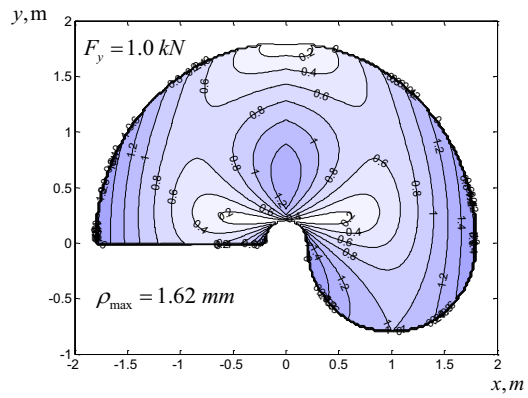

(d) Compliance map for *quasi-serial manipulator* under the external loading in y-direction

Figure 5. Compliance error maps for serial and quasi-serial manipulators under different external loadings (F_x and F_y)

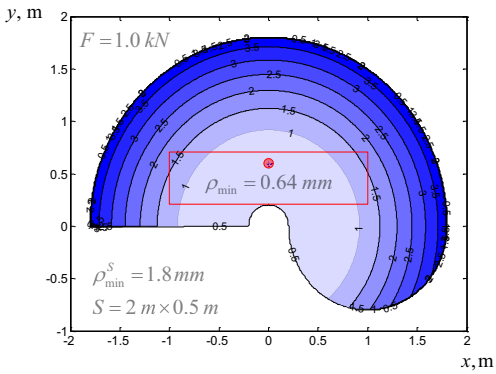

(a) Maximum compliance errors for arbitrary force directions for *serial manipulator*

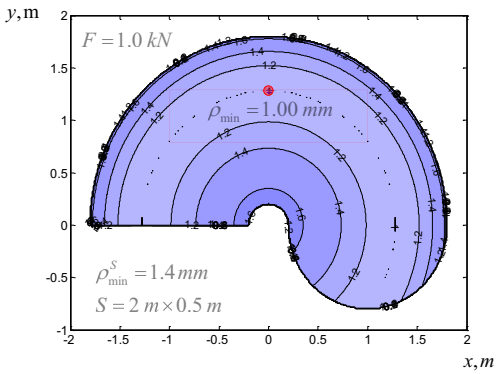

(b) Maximum compliance errors for arbitrary force directions for *quasi-serial manipulator*

Figure 6. Maximum compliance errors for serial and quasi-serial manipulators: case of arbitrary force direction

5 Comparison of compliance errors for serial and quasi-serial manipulators

To demonstrate advantages/disadvantages of both serial and quasi-serial architectures, let us present an example showing that the selection of a proper manipulator type essentially depends on the technological task dimension and external force orientation. This example deals with two manipulators (serial and quasi-serial ones) with the same geometric parameters $l_2 = 1m$, $l_3 = 0.8m$ and identical joint compliances $k = 10^{-6}\ N\,m\,/\,rad$. These values are typical for industrial robots that are used in machining applications. To compare their stiffness behaviour, let us compute the compliance errors caused by an external force 1.0 *kN* which is applied to the end-effector. Relevant results have been obtained for two different external loadings (applied in x- and y-directions). They are presented in Fig. 5, which shows the compliance error distribution within the manipulator workspace for both serial and quasi-serial robots.

As follows from the result presented in Fig. 5, the elastostatic deflections for the serial manipulator vary through the workspace and may reach up to 3.83 mm. For the quasi serial manipulator, the upper value is 1.62 mm. These results show that for the considered case study the compliance errors range does not depend on the force direction, while the compliance error maps of the two manipulators are not identical. It should be also

mentioned that for both manipulators the best accuracy is achieved at the workspace boundary (i.e., in a singular configuration), which is not acceptable in the most of industrial applications. Moreover, at the corresponding workspace points, the compliance error achieves its maximum value for the orthogonal force direction.

To compare the considered architectures, let us first find the workspace point, which provides the smallest compliance errors for all possible force directions. It is clear that in the neighbourhood of this point it is reasonable to locate a technological task of relatively small dimensions. The relevant computations demonstrated that the minimum compliance errors are 0.64 and 1.00 mm for the serial and quasi-serial robots respectively (Fig. 6). Hence, the serial architecture is preferable for small-dimensional tasks.

Further, let us locate in the manipulator workspace a technological task of size 0.5×2 m, which can be treated as a large-dimensional one (compared to the manipulator workspace). Corresponding computational results show that the minimum compliance errors that can be achieved for all possible force directions and for all task points are 1.8 mm and 1.4 mm for the serial and quasi-serial manipulators correspondingly. Hence, the quasi-serial architecture is preferable for the large-dimensional tasks.

6 Conclusions

The paper deals with comparison analysis of serial and quasi-serial manipulators. The obtained results show that the quasi-serial manipulators are preferable for large-dimensional tasks, while the serial ones better suit small and medium size tasks, assuming that the machining task is optimally located within the robot workspace. When the task location is predefined and cannot be optimized, the quasi-serial manipulators should be used since they provide more homogenous compliance error distribution within the entire robot workspace. Another advantage of the quasi-serial manipulators is related to the fact that the best accuracy is ensured in the mid-workspace, while the compliance errors minimum for the serial manipulators is achieved on the workspace boundary.

Acknowledgments

The work presented in this paper was partially funded by the project Partenariat Hubert Curien SIAM 2016 France-Thailand.

References

1. Chérif, M., et al., Generic modelling of milling forces for CAD/CAM applications. International Journal of Machine Tools and Manufacture, 2004. 44(1): p. 29-37.
2. Vosniakos, G.-C. and E. Matsas, Improving feasibility of robotic milling through robot placement optimisation. Robotics and Computer-Integrated Manufacturing, 2010. 26(5): p. 517-525.
3. Guo, Y., et al., Vibration analysis and suppression in robotic boring process. International Journal of Machine Tools and Manufacture, 2016. 101: p. 102-110.
4. Klimchik, A., et al., Compliance error compensation technique for parallel robots composed of non-perfect serial chains. Robotics and Computer-Integrated Manufacturing, 2013. 29(2): p. 385-393.
5. Chen, Y., et al., Spatial statistical analysis and compensation of machining errors for complex surfaces. Precision Engineering, 2013. 37(1): p. 203-212.
6. Drouet, P., et al., Compensation of geometric and elastic errors in large manipulators with an application to a high accuracy medical system. Robotica, 2002. 20(03): p. 341-352.
7. Klimchik, A., et al. Identification of geometrical and elastostatic parameters of heavy industrial robots. in IEEE International Conference on Robotics and Automation (ICRA) 2013.
8. Klimchik, A., et al., Optimal Selection of Measurement Configurations for Stiffness Model Calibration of Anthropomorphic Manipulators. Applied Mechanics and Materials, 2012. 162: p. 161-170.
9. Belchior, J., et al., Off-line compensation of the tool path deviations on robotic machining: Application to incremental sheet forming. Robotics and Computer-Integrated Manufacturing, 2013. 29(4): p. 58-69.
10. Guo, Y., et al., A multilevel calibration technique for an industrial robot with parallelogram mechanism. Precision Engineering, 2015. 40: p. 261-272.
11. Sun, Y. and J.M. Hollerbach. Observability index selection for robot calibration. in Robotics and Automation, 2008. ICRA 2008. IEEE International Conference on. 2008.
12. Klimchik, A., et al., Geometric and elastostatic calibration of robotic manipulator using partial pose measurements. Advanced Robotics, 2014. 28(21): p. 1419-1429.
13. Imoto, J., et al., Optimal kinematic calibration of robots based on maximum positioning-error estimation (Theory and application to a parallel-mechanism pipe bender), in Computational Kinematics. 2009, Springer. p. 133-140.
14. Wu, Y., et al., Geometric calibration of industrial robots using enhanced partial pose measurements and design of experiments. Robotics and Computer-Integrated Manufacturing, 2015. 35: p. 151-168.
15. Yan, S.J., S.K. Ong, and A.Y.C. Nee, Stiffness analysis of parallelogram-type parallel manipulators using a strain energy method. Robotics and Computer-Integrated Manufacturing, 2016. 37: p. 13-22.
16. Klimchik, A., D. Chablat, and A. Pashkevich, Stiffness modeling for perfect and non-perfect parallel manipulators under internal and external loadings. Mechanism and Machine Theory, 2014. 79: p. 1-28.
17. Quennouelle, C. and C.m. Gosselin. Instantaneous kinemato-static model of planar compliant parallel mechanisms. in ASME 2008 International Design Engineering Technical Conferences and Computers and Information in Engineering Conference. 2008. American Society of Mechanical Engineers.
18. Pashkevich, A., A. Klimchik, and D. Chablat, Enhanced stiffness modeling of manipulators with passive joints. Mechanism and machine theory, 2011. 46(5): p. 662-679.
19. Klimchik, A., et al., Identification of the manipulator stiffness model parameters in industrial environment. Mechanism and Machine Theory, 2015. 90: p. 1-22.
20. Nubiola, A. and I.A. Bonev, Absolute calibration of an ABB IRB 1600 robot using a laser tracker. Robotics and Computer-Integrated Manufacturing, 2013. 29(1): p. 236-245.